Macroscopic bursting in physiological networks: node or network property?

Ferrari, F A S ; Gomez, F ; Lorimer, T ; Viana, R L ; Stoop, R

DOI: https://doi.org/10.1088/1367-2630/17/5/055024

Macroscopic bursting in physiological networks: node or network property?

2015 New J. Phys. 17 055024

New Journal of Physics
The open access journal at the forefront of physics

Deutsche Physikalische Gesellschaft DPG
IOP Institute of Physics

Published in partnership with: Deutsche Physikalische Gesellschaft and the Institute of Physics

OPEN ACCESS

RECEIVED
13 February 2015

REVISED
16 April 2015

ACCEPTED FOR PUBLICATION
28 April 2015

PUBLISHED
27 May 2015

PAPER

Macroscopic bursting in physiological networks: node or network property?

Fabiano A S Ferrari[1], **Ricardo L Viana**[1,3], **Florian Gomez**[2], **Tom Lorimer**[2] **and Ruedi Stoop**[2,4]

[1] Physics Department, Federal University of Paraná, 81531-990, Curitiba, Brazil
[2] Institute of Neuroinformatics and Institute of Computational Science, University and ETH of Zurich, 8057 Zurich, Switzerland
[3] http://fisica.ufpr.br/viana/
[4] http://stoop.ini.uzh.ch/

E-mail: viana@fisica.ufpr.br **and** ruedi@ini.phys.ethz.ch

Keywords: neurons, networks, bursting

Abstract

Activity pattern modalities of neuronal ensembles are determined by node properties as well as network structure. For many purposes, it is of interest to be able to relate activity patterns to either node properties or to network properties (or to a combination of both). When in physiological neural networks we observe bursting on a coarse-grained time and space scale, a proper decision on whether bursts are the consequence of individual neurons with an inherent bursting property or whether we are dealing with a genuine network effect has generally not been possible because of the noise in these systems. Here, by linking different orders of time and space scales, we provide a simple coarse-grained criterion for deciding this question.

1. Introduction

Neuronal bursting activity is a ubiquitous physiological state described by a precipitate train of spikes followed by a quiescent period. The phenomenon can be observed on the node or on the network level, and it can be produced by neurons bursting by their own virtue ('inherent bursting') or by neurons that individually respond with regular spiking but exhibit a bursting behavior when embedded as a node into a network (possibly conditional on a particular input to the network that drives the latter into a particular functional mode). Bursting has several distinct functional roles. Within the neocortex's layer IV, bursting activity emerges as a collective phenomenon [1], enabling the amplification of weak thalamic input into the network. In neuronal embryonic cultures, we generally observe bursting activity after a few days of implementation, when the neuronal network starts to develop its structure. In this case, bursting is the fingerprint of the search by the network for its optimal configuration, which is indicated by an avalanche structure of the firing events (see figure 1), the size of which has a power-law characteristic [2–5]. The most obvious instance of a functional role of bursting is the neuronal contact to muscles, where bursting is required for muscle contraction [6]. Besides that, frequency features of bursting neurons have also been shown to be important due to their resonant properties, which allow them to transmit reliably selective information between neuronal circuits [7, 8]. Not least, bursting or synchronized activity hallmarks a number of important conditions in human health, as it has been shown to be closely related, e.g., to the emergence of epilepsy [9] and migraine [10] and to pacemaker function [11].

The experimental situation that we focus on in our investigation is a coarse-grained, macroscopic one, where we have no microscopic access to individual neuronal spiking or where we have too many elements to deal with on an individual basis. We will show that the two main alternatives that lead to bursting produce different effects on the network level (that may have physiological relevance), and we will provide a mixed qualitative and quantitative analysis of the difference between the two situations. As bursting is an intrinsically nonlinear phenomenon, we compare two extreme cases of nonlinear models: the weak nonlinear coupling of linear phase oscillators (Kuramoto case [12, 13]) and the coupling of intrinsically nonlinear oscillators ('Rulkov neurons' [14]). Because of their distinguished position among the extant models of neuronal dynamics, both have been

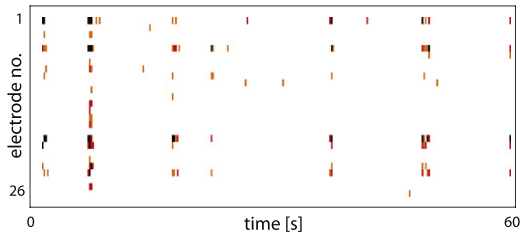

Figure 1. Mesoscopic observation of bursting in embryonic cultures grown on a chip (data: courtesy of the Y. Nam Lab, KAIST, Daejeon). Colors code for the 'number of spikes per bin' (200 ms). 1 spike: orange, 2–3 spikes: red, 4 or more: black.

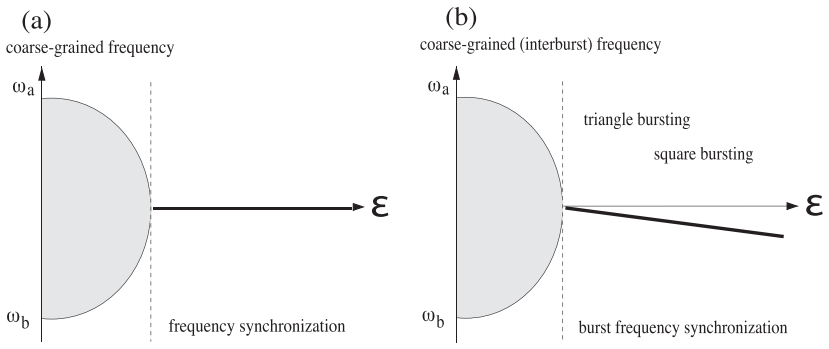

Figure 2. Scheme of the frequency distributions obtained for globally coupled networks on the coupling strength ε: (a) Kuramoto phase oscillators, and (b) Rulkov neurons. For each ε, the simulation started with an ensemble of nodes sampled from an interval (ω_a, ω_b) hosting a unimodal symmetric frequency distribution.

abundantly used for modeling neurons and neuronal networks. Authoritative surveys and examples of their potential use for these tasks are provided, e.g., in [15, 16] for the Kuramoto model and in [17, 18] for the Rulkov model. Due to their prominence, it is, unfortunately, impossible to do justice to the vast literature available. As Rulkov's model recovers essentially all behaviors of neuronal firing observed in physiology (even regular firing), we may see it as the generic nonlinear model covering the whole of the modeling space, beyond simple phase oscillators onwards to the strongly nonlinear behavior of bursting neurons.

Bursting is characterized in all cases by two time scales: a fast one responsible for individual spiking and a slow one responsible for bursting. From a macroscopic and large time-scale point of view, a regular interburst interval between two successive bursts can be considered as the correspondence to one complete oscillation of a regular neuron; i.e., the burst is considered as a single event. The interburst frequency will then be defined by the number of bursts per unit time. In this sense, a phase θ can be associated with the angular position of an equivalent rotating oscillator, and the interburst angular frequency ω is the average of the angular frequencies evaluated over some time series. When coupled, inherently bursting neurons are able to show regular firing and phase synchronization [14]. Based on this, the emergence of neuronal phase synchronization can be seen as equivalent to the mechanism of phase synchronization for coupled Kuramoto oscillators. Regarding phase dynamics, an explicit mapping between the Rulkov model within a given regime of firing, and the Kuramoto model was recently developed [19]. We will see that, surprisingly, this no longer holds if we, instead, consider frequency as the observable; the frequency ω of coupled bursting neurons and the frequency of Kuramoto oscillators depend distinctively on the coupling strength between the neurons.

In contrast to synchronized coupled Kuramoto oscillators, where the coarse-grained frequency (that often displays burst-like characteristics) does not vary with coupling strength (figure 2(a)), for synchronized coupled inherently bursting Rulkov neurons, the mean interburst frequency (MIF) *decreases* if the coupling strength ε is increased. This unexpected response of inherently bursting neurons is corroborated by physiological observations of coupled pyloric dilator neurons from the lobster stomatogastric ganglion. (For these neurons, it is well known that when they are coupled with artificial electrical synapses, their MIF changes with the coupling strength [20].) One aim of this paper is to explain this unexpected behavior and to exhibit that for the modeling of certain collective neuronal phenomena, the choice of phase oscillators for node dynamics may be insufficient. To work these points out, we first closely follow and then extend to some point the original analysis provided by Rulkov [14].

2. Frequency dependence of synchronizing Kuramoto neurons

We first recollect how the emergent macroscopic frequency depends on the coupling for the prominent Kuramoto oscillator model of neurons (i.e., weakly coupled linear phase oscillators). It is well known [13] that increased coupling among the oscillators leads to the emergence of synchronized phase behavior. For our investigations, the frequency of oscillation ω_i of the oscillator θ_i, $i = 1,\ldots, N$, where N is the network size, will be chosen randomly from a symmetric and unimodal probability density function $g(\omega)$, and the coupling that we shall consider is global:

$$\dot{\theta}_i = \omega_i + \frac{\varepsilon}{N}\sum_{j=1}^{N}\sin\left(\theta_j - \theta_i\right). \tag{1}$$

($\dot{\theta}_i$ is the temporal phase evolution of the ith neuron, and ε is the global coupling strength.) For the simplest case of the coupling of two oscillators (for the earliest experiments regarding biological neurons see [21, 22]), we may perform the transformation $\varphi = \theta_2 - \theta_1$ so that $\dot{\varphi} = (\omega_2 - \omega_1) - \varepsilon\,\sin(\varphi)$ and consider the condition to frequency synchronization $\dot{\varphi} = 0$. Frequency synchronization will be achieved for $\varepsilon > \varepsilon_c = \omega_2 - \omega_1$ at mean frequency $\Omega = (\omega_1 + \omega_2)/2$ for all values of the coupling strength $\varepsilon > \varepsilon_c$ [23, 24]. Although for a larger number of oscillators the analytics become increasingly difficult [25], it is known that the frequency average of the coupled Kuramoto oscillators continues to be the average frequency of the uncoupled Kuramoto oscillators, where this property is independent of network topology and network size. This invariance of the mean frequency of Kuramoto oscillators is, however, for most modeling of physiological systems, an unrealistic limitation.

3. Burst-frequency dependence of Rulkov neurons

Most physiological ensembles of neurons that undergo a synchronization process also contain neurons with inherent bursting behavior. (As we will see, neurons may also change from regular to bursting behavior, depending on physiological conditions.) A generic and convenient framework of neurons with different physiological responses is given by Rulkov's two-dimensional (2D) map [14] based on a fast x-variable and a slow y-variable,

$$x_{n+1} = \frac{\alpha}{(1 + x_n^2)} + y_n, \tag{2}$$

$$y_{n+1} = y_n - \sigma x_n - \beta, \tag{3}$$

where n is the discrete time step, α is the nonlinearity parameter, and β and σ are complementary parameters. Upon the variation of the parameter α (that may be associated with physiological influences), this model can assume very different types of neuronal activity (figures 3(a)–(d)). Fixing $\beta = \sigma = 0.001$, for $\alpha \lesssim 2.0$ the model shows a quiescent behavior (figure 3(a)), whereas for $2.0 \lesssim \alpha \lesssim 2.58$, regular spikes are observed (figure 3(b)). For $\alpha \gtrsim 2.58$ we are in the burst regime. The latter regime is divided into two sub-regimes: 'triangle bursting' occurs if $2.58 \lesssim \alpha < 4.0$ (figure 3(c)); and 'square bursting' occurs if $4.0 < \alpha \lesssim 4.62$ (figure 3(d)).

The different behaviors are naturally associated with different relationships between the slow and the fast dynamics of the model. For high values of α ($\alpha \gtrsim 2.58$) the y-variable (red lines in figures 3(a)–(d)) varies slowly in comparison to the x-variable (black lines in figures 3(a)–(d)). Through a decomposition of the fast from the slow time-scale, it is possible to arrive from the 2D system at a 1D system, where the slow variable is replaced by the parameter γ as

$$x_{n+1} = \alpha/(1 + x_n^2) + \gamma. \tag{4}$$

This dimensional reduction simplifies the bifurcation analysis [14]. As we shall see, the behavior of the 2D system is well described by the simplified system. The gray region in figure 4 shows the accessible parameter space for the 2D Rulkov model. The reduced Rulkov model hosts three important dynamical features: a saddle-node bifurcation, a flip bifurcation, and a crisis [26]. The saddle-node bifurcation, which consists in a collision between a stable and an unstable fixed point, occurs when the following four conditions are satisfied: (i) $F(x_0) = x_0$; (ii) $\frac{\partial F(x_0,\gamma_0)}{\partial x} = 1$; (iii) $\frac{\partial F(x_0,\gamma_0)}{\partial \gamma} \neq 0$; and (iv) $\frac{\partial^2 F(x_0,\gamma_0)}{\partial x^2} \neq 0$ [27]. From equation (4) for $F(x_0, \gamma_0)$, the α and γ that satisfy the four conditions are given by the relation

$$\alpha = (-18\gamma - 2\gamma^3 \pm 2(\gamma^2 - 3)^{3/2})/27. \tag{5}$$

This relation is represented in figure 4 by a full black line. The flip bifurcation is caused if an unstable fixed point and a stable orbit of period two merge into one single fixed point. The four conditions that must be fulfilled in this case are (i) $F(x_0) = x_0$; (ii) $\frac{\partial F(x_0,\gamma_o)}{\partial x} = -1$; (iii) $\frac{\partial F(x_0,\gamma_0)}{\partial \gamma} \neq 0$; and (iv) $\frac{\partial^2 F(x_0,\gamma_0)}{\partial x^2} \neq 0$ [28]. In this case α and γ must obey the relation

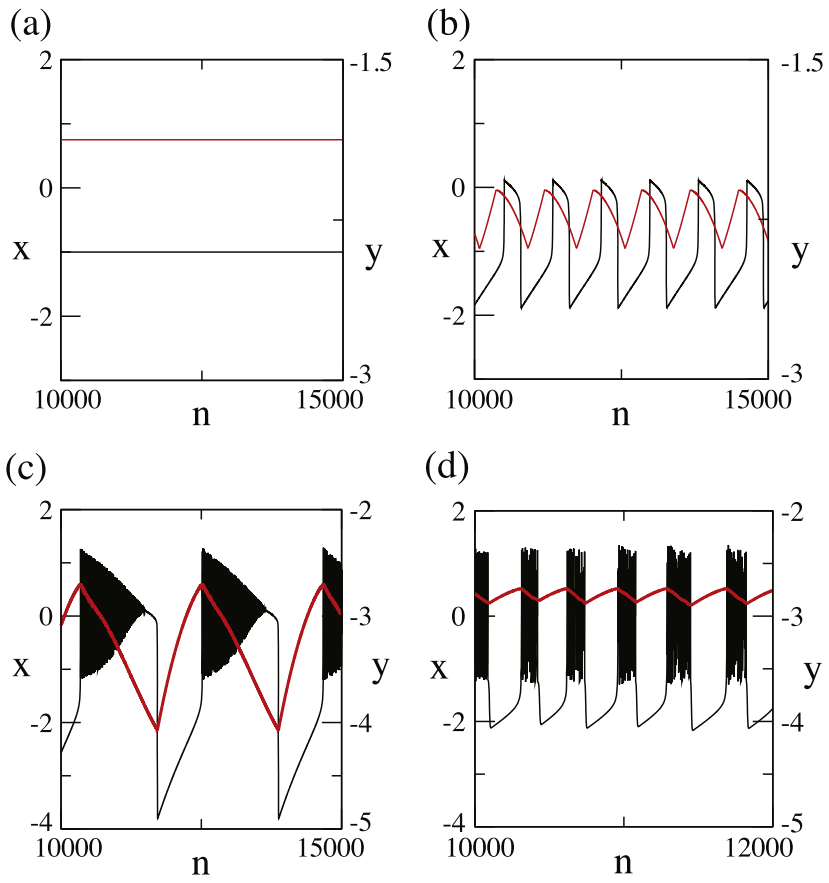

Figure 3. Neuronal activity of Rulkov neurons depending on α parameter: (a) quiescent, $\alpha = 1.75$; (b) periodic spike, $\alpha = 2.25$; (c) triangle-burst, $\alpha = 3.99$; and (d) square-burst, $\alpha = 4.1$. Black lines represent the x-variable (left-hand side units) and the red lines represent the y-variable (right-hand side units). n numbers the discrete iteration steps of the model.

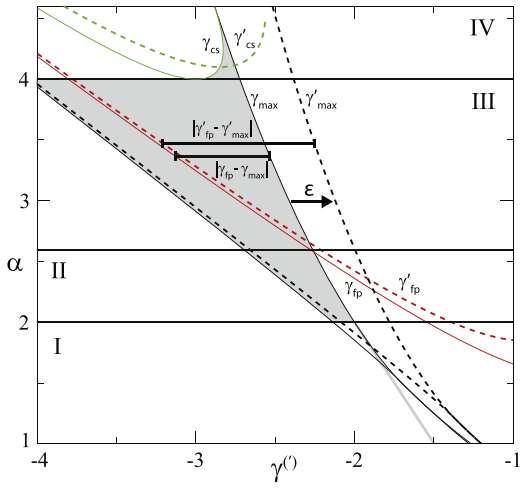

Figure 4. Parameter space for the 1D Rulkov model (full lines: uncoupled case ($\varepsilon = 0$), dashed lines and dashed parameter: globally coupled case ($\varepsilon = 0.2$)). Black: saddle-node bifurcation points, red: flip bifurcation points, green: crisis points. Full horizontal lines delimit the different regions I–IV of neuronal activity for $\varepsilon = 0.0$. The gray background indicates the space accessible by the 2D Rulkov map. The horizontal arrow indicates the effect by the coupling of neurons on the rhs. boundary. (The lhs boundary basically remains at its location.)

$$\alpha = 2\gamma^3 \pm 2(1+\gamma^2)\sqrt{\gamma^2+1}\,, \tag{6}$$

which is represented in figure 4 by a full red line. A crisis is a sudden change in the chaotic attractor (here: its disappearance). This happens if the maximum of function $F(x)$ is mapped into a stable fixed point [29]. This condition is satisfied if the relation

$$\alpha = \left(-3\gamma \pm \sqrt{\gamma^2 - 8} \right) \Big/ 2 \tag{7}$$

holds, which is represented in figure 4 by the full green line.

From the bifurcations of the reduced Rulkov model, we may understand how the individual dynamics separates into different regimes. Whereas for $\alpha \lesssim 2.0$ the x- and y-trajectories will be attracted to a fixed point (region I in figure 4), for $2.0 \lesssim \alpha \lesssim 2.58$ the y-variable will oscillate between two saddle-node bifurcation points, and the x-variable will be confined to a periodic motion (region II in figure 4). For $2.58 \lesssim \alpha < 4.0$ we have coexistence of the saddle-node bifurcation and of the flip bifurcation points, which produces the triangle bursting. In this case, when the y-variable reaches the largest saddle-node bifurcation point ($\gamma_{\max}$), the x-variable starts to oscillate rapidly as the y-variable decreases towards the flip bifurcation point (γ_{fp}), and the amplitude of the oscillation decreases. When the fast oscillations disappear, the bursting terminates, and the trajectory is attracted to the fixed point. After the orbit reaches the stable fixed point, the y-variable slowly increases towards $\gamma_{\max}$, which completes the loop (region III in figure 4). The square bursting happens if $4.0 < \alpha \lesssim 4.62$: in this case the y-variable grows up to $\gamma_{\max}$. At this point, a chaotic attractor emerges, and the y-variable decreases towards the crisis point (γ_{cs}). At this point the chaotic attractor vanishes, and, consequently, bursting is terminated. After that, the orbit is attracted by the stable fixed point, and the y-variable increases its value towards $\gamma_{\max}$ again (region IV in figure 4).

Already in Rulkov's original paper [14], a hint can be found that in some area of the parameter space, ω might be basically inversely proportional to the distance $|\gamma_{fp} - \gamma_{\max}|$. However, no indication was given as to whether this holds generally, or for what network topologies this would be the case. We infer from figure 4 that if the argument holds, then the strength of ε may have a noticeable impact on the burst frequency ω. To pinpoint this, we numerically simulated different network topologies (for diffusive coupling, small-world networks, and scale-free networks) that all exhibit essentially identical behavior. In this paper, though, we restrict ourselves to the case of globally coupled networks. A burst starts whenever $y_n = \gamma_{\max}$. Defining the oscillation period as the time between the beginning of two successive bursts, we obtain a corresponding phase (φ) as

$$\varphi_n = 2\pi k + \frac{2\pi (n - n_k)}{(n_{k+1} - n_k)} \quad (n_k < n < n_{k+1}), \tag{8}$$

where n_k now indicates the time at which the kth burst starts. For the definition of MIF we use an extension of the usual rotation number

$$\omega = \lim_{n' \to \infty} \frac{(\varphi_{n=n'} - \varphi_{n=0})}{n'}. \tag{9}$$

As is shown in figure 5(a), in the triangle-bursting regime, the distance between the flip bifurcation point (γ_{fp}) and $\gamma_{\max}$ increases linearly in α. ω, being inversely proportional to the distance between these two points, $\omega \propto |\gamma_{fp} - \gamma_{\max}|^{-1}$, thus decreases (figures 5(b) and (c)). If we increase α within the square-bursting regime, the distance between the crisis bifurcation point γ_{cs} and $\gamma_{\max}$ decreases. The mean interburst frequency thus increases until, towards the end of the square-bursting regime, the proximity to another regime of neuronal activity at $\alpha = 8\sqrt{3}/3 \approx 4.62$, and the small distance between the bifurcation points causes other types of modulations that for the interburst frequency become relevant, forcing MIF to decay again.

We proceed from the single-neuron case to the collective behavior by investigating the behavior of a globally coupled set of Rulkov neurons

$$\begin{aligned} x_{n+1}^{(i)} &= \alpha \Big/ \left(1 + \left(x_n^{(i)} \right)^2 \right) + y_n^{(i)} + \frac{\varepsilon}{N} \sum_{j=1}^{N} x_n^{(j)}, \\ y_{n+1}^{(i)} &= y_n^{(i)} - \eta \left(x_n^{(i)} - \sigma \right), \end{aligned} \tag{10}$$

where ε is the coupling strength, N is the network size, and $i = 1, \ldots, N$. Also for synchronized Rulkov neurons, a reduction of the 2D model to a 1D model is possible, so that

$$x_{n+1} = \alpha/(1 + x_n^2) + \gamma' + \varepsilon x_n. \tag{11}$$

We may now use the same arguments that we have used for isolated Rulkov neurons. The critical points for global coupling corresponding to equations (5)–(7) are given by (see [26] for more details)

$$\alpha = \frac{-18\gamma'(1-\varepsilon)^2 - 2\gamma'^3 \pm (2\gamma'^2 - 6(1-\varepsilon)^2)\sqrt{\gamma'^2 - 3(1-\varepsilon)^2}}{27(1-\varepsilon)^2}, \tag{12}$$

$$\alpha = \frac{-18\gamma'\varepsilon^3 + 18\gamma'\varepsilon^2 + 2\gamma'\varepsilon - 2\gamma'^3\varepsilon - 2\gamma'^3 - 2\gamma'}{(3\varepsilon - 1)^3} \tag{13}$$

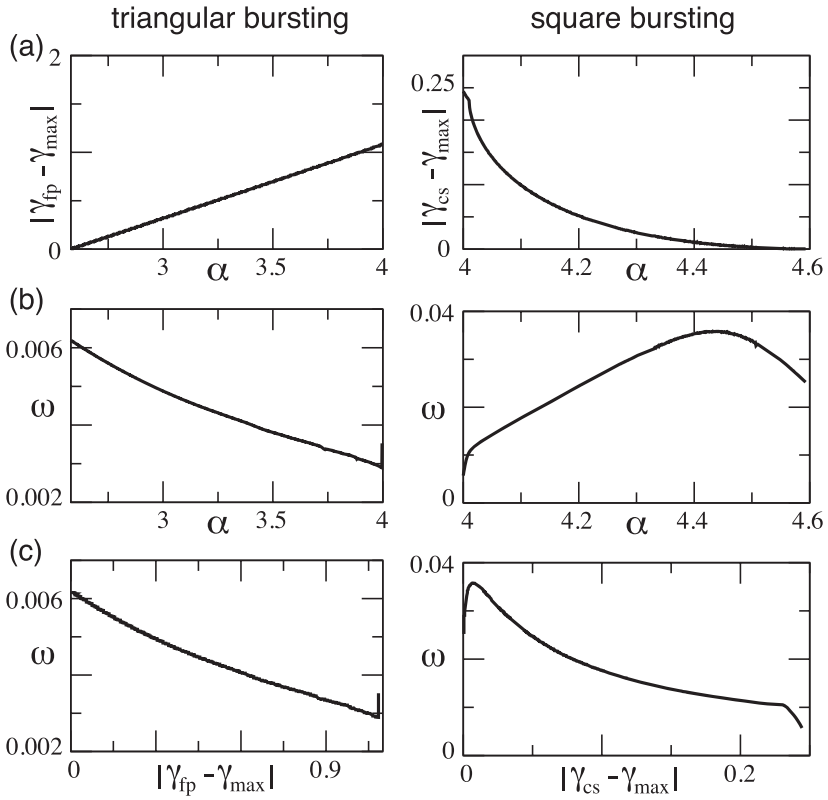

Figure 5. Frequency dependence of uncoupled Rulkov maps in the two regions of bursting. (a) Relation between bifurcation point distance $|\gamma_{fp} - \gamma_{\max}|$ and α parameter. (b) Relation between the mean interburst frequency (ω) and α parameter. (c) Relation between mean interburst frequency and bifurcation point distance $|\gamma_{cs} - \gamma_{\max}|$ ($\sigma = \beta = 0.001$).

$$\pm \frac{(2\gamma'^2\varepsilon + 14\varepsilon^2 - 10\varepsilon + 2 + 2\gamma'^2 - 6\varepsilon^3)\sqrt{\gamma'^2 - (\varepsilon + 1)(3\varepsilon - 1)}}{(3\varepsilon - 1)^3},$$

$$\alpha = \frac{-\gamma' \pm \sqrt{\gamma'^2 - 4((1-\varepsilon)^2 + 1)}}{2(1-\varepsilon)^2} - \gamma', \tag{14}$$

where equation (12) provides the saddle-node bifurcation points $\gamma'_{\max}$, equation (13) the flip bifurcation points γ'_{fp}, and equation (14) the crisis points γ'_{cs}. According to figure 4, while the coupling increases from $\varepsilon = 0$ (full lines) to $\varepsilon = 0.2$ (dashed lines), there is a displacement of the bifurcation lines and, as consequence, a change in the MIF. It is now evident that increased coupling increases the distance between the bifurcation points (figure 6(a)). For triangle bursting, MIF decreases almost linearly with the coupling and decreases for square bursting with an approximately quadratic dependence (figure 6(b)). While the dependence between frequency and bifurcation point distances decreases in an approximately linear manner for triangle bursting, for square bursting the decrease is nonlinear (figure 6(c)).

These results demonstrate that, indeed, inside a given neuronal activity regime (triangle bursting, square bursting), the increase of the distance between the bifurcation points in consequence of an increase of ε (or of α), decreases the interburst frequency ω. This dependence is observed at the neuronal level (figure 5(c)), as well as if the neurons are coupled (figure 6(c)). If the increase (or decrease) of the coupling strength is too big, there will be additional, non-continuous changes in neuronal activity. Abrupt changes can be seen upon a change between activity regimes, e.g., when, upon the increase of α, we change from triangle bursting into square bursting (figure 5(b)), or in dependence of the coupling strength.

The difference between the simple dependence on the coupling strength ε by the Kuramoto model versus the essentially strictly monotonous dependence interrupted by events of bifurcations exhibited by Rulkov neurons should therefore be seen as the hallmark of a preponderance of inherently versus non-inherently bursting neurons.

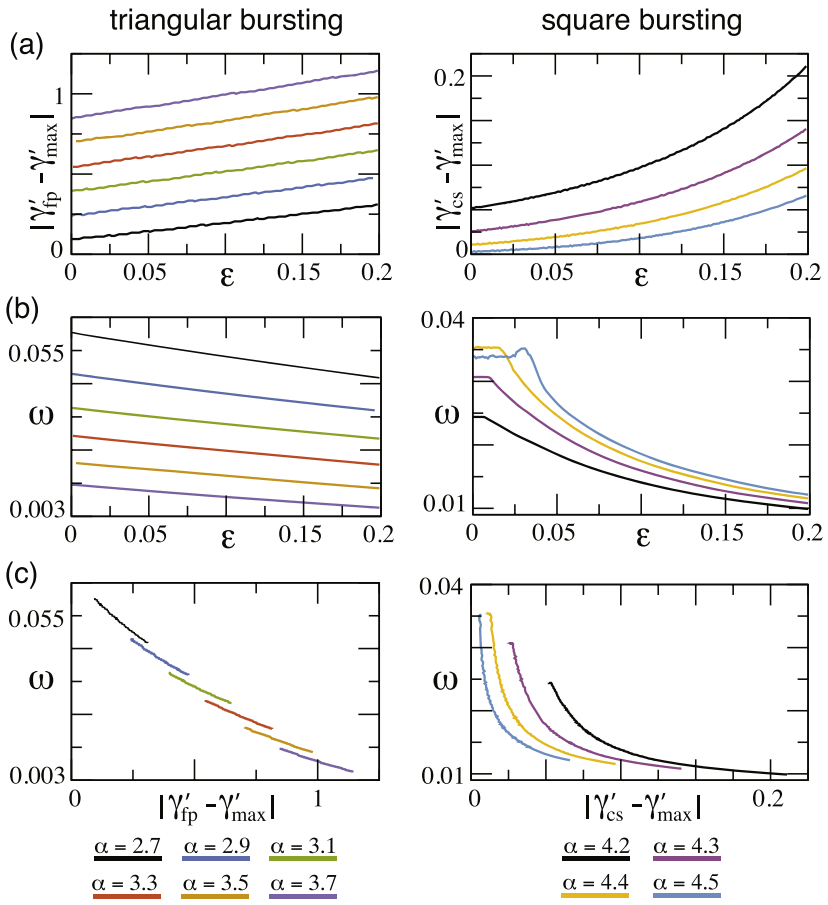

Figure 6. Frequency dependence of globally coupled Rulkov neurons in the two regions of bursting. (a) Relation between bifurcation point distance and the coupling strength ε. (b) Relation between the mean burst frequency ω and coupling strength ε. (c) Relation between mean bursting frequency and bifurcation point distance. Size of networks: $N = 1000$.

4. Conclusions

Despite the differences between the Rulkov and Kuramoto neuron models, in the periodic regime $2.0 \lesssim \alpha \lesssim 2.58$ the coupling effect in the spike frequency can be neglected, and the Kuramoto model can be used to model phase and frequency synchronization. In the bursting regime of neurons, $\alpha \gtrsim 2.58$, the differences between the models matter, as for inherently bursting neurons, consistently a decrease of MIF with the coupling strength was observed for global, small-world, and scale-free topologies of sizes varying from $N = 100$ up to $N = 10000$. Related observations made earlier for different systems ([30] for diffusive coupling, [31] for small-world networks, and [32] for scale-free networks) corroborate the interpretation that our observation deals with a general feature of inherently bursting neurons. We have focused on the MIF of Rulkov's model of bursting neurons. This should, however, not be considered a particular modeling case, but rather as a generic framework that reflects dynamical properties essential for both regular and bursting behavior. Neurons that can become inherently bursting may therefore be the more typical case than neurons that do not offer this possibility. The dependence of the MIF on the coupling exhibited by these neurons (figure 6) then would (at least in matters of frequency) prohibit a modeling by simple phase oscillators, which still is the predominant approach. The apparent independence of the observed phenomenon with respect to network topology makes it a rare example of a nontrivial invariant of network topology.

In view of the exhibited different origins that can underlie bursting, we suggest that our observation will be helpful on different levels of physiological coarse-graining. Particularly on higher levels of abstraction of the representation of physiology (i.e., working with higher levels of modularity), it will be to a lesser degree evident whether for modeling subsystems, a phase oscillator model suffices, or whether a bursting model is necessary. Our results provide a simple experimentally accessible indicator for deciding this question. It is conceivable that for neuronal networks with well-controlled architecture, experimental procedures (e.g., the addition of serotonin or related substances) could be developed to mimic an increase or decrease of the coupling strength ε

among the nodes of a biological neural network, obtaining in this way the desired information about the dominant nature of the nodes.

Traditionally, most emphasis in the analysis of complex physiological networks has been dedicated to the microscale and the macroscale. Our results, however, put a warning sign against too straightforward an extrapolation from a microscopic level to the macroscopic scale: mesoscale effects, such as the pattern of bursting investigated here from this angle, can generate quite unexpected effects that can cause these extrapolations to fail. This implies that increased efforts on the mesoscale will be necessary to better understand physiological neuronal systems that span different levels of hierarchical organization.

Acknowledgments

This work was made possible by financial support to FF from the Brazilian Research Agencies, from Coordination for the Improvement of Higher Education Personnel (Brazil) (CAPES) and from National Council for Scientific and Technological Development (Brazil) (CNPq).

References

[1] Stoop R, Blank D, Kern A, Vyver J J, Christen M, Lecchini S and Wagner C 2002 Collective bursting in layer iv synchronization by small thalamic inputs and recurrent connections *Cognitive Brain Res.* **13** 293–304
[2] Beggs J M and Plenz D 2003 Neuronal avalanches in neocortical circuits *J. Neurosci.* **23** 11167–77
[3] Beggs J M and Plenz D 2004 Neuronal avalanches are diverse and precise activity patterns that are stable for many hours in cortical slice cultures *J. Neurosci.* **24** 5216–29
[4] Levina A, Herrmann J M and Geisel T 2009 Phase transitions towards criticality in a neural system with adaptive interactions *Phys. Rev. Lett.* **102** 118110
[5] de Arcangelis L and Herrmann H J 2010 Learning as a phenomenon occurring in a critical state *Proc. Natl Acad. Sci. USA* **107** 3977–81
[6] Birmingham J T, Szuts Z B, Abbott L F and Marder E 1999 Encoding of muscle movement on two time scales by a sensory neuron that switches between spiking and bursting modes *J. Neurophysiol.* **82** 2786–97
[7] Lisman J E 1997 Bursts as a unit of neural information: making unreliable synapses reliable *Trends Neurosci.* **20** 38–43
[8] Izhikevich E M, Desai N S, Walcott E C and Hoppensteadt F C 2003 Bursts as a unit of neural information: selective communication via resonance *Trends Neurosci.* **26** 161–7
[9] Lehnertz K and Elger C E 1998 Can epileptic seizures be predicted? Evidence from nonlinear time series analysis of brain electrical activity *Phys. Rev. Lett.* **80** 5019
[10] Angelini L *et al* 2004 Steady-state visual evoked potentials and phase synchronization in migraine patients *Phys. Rev. Lett.* **93** 038103
[11] Verheijck E E, Wilders R, Joyner R W, Golod D A, Kumar R, Jongsma H J, Bouman L N and van Ginneken A C 1998 Pacemaker synchronization of electrically coupled rabbit sinoatrial node cells *J. Gen. Physiol.* **111** 95–112
[12] Kuramoto Y 1975 Self-entrainment of a population of coupled non-linear oscillators *Lect. Notes Phys.* **39** 420–2
[13] Strogatz S H 2000 From Kuramoto to Crawford: exploring the onset of synchronization in populations of coupled oscillators *Physica* D **143** 1–20
[14] Rulkov N F 2001 Regularization of synchronized chaotic bursts *Phys. Rev. Lett.* **86** 183–6
[15] Acebrón J A, Bonilla L L, Vicente C J P, Ritort F and Spigler R 2005 The Kuramoto model: a simple paradigm for synchronization phenomena *Rev. Mod. Phys.* **77** 137–85
[16] Cumin D and Unsworth C P 2007 Generalising the Kuramoto model for the study of neuronal synchronisation in the brain *Physica* D **226** 181–96
[17] Rulkov N F, Timofeev I and Bazhenov M 2004 Oscillations in large-scale cortical networks: Map-based model *J. Comput. Neurosci.* **17** 203–23
[18] Ibarz B, Casado J M and Sanjuán M A 2011 Map-based models in neuronal dynamics *Phys. Rep.* **501** 1–74
[19] Ferrari F A S, Viana R L, Lopes S R and Stoop R 2015 Phase synchronization of coupled bursting neurons and the generalized Kuramoto model *Neural Netw.* **66** 107–18
[20] Elson R C, Selverston A I, Huerta R, Rulkov N F, Rabinovich M I and Abarbanel H D I 1998 Synchronous behavior of two coupled biological neurons *Phys. Rev. Lett.* **81** 5692
[21] Stoop R, Schindler K and Bunimovich L A 2000 When pyramidal neurons lock, when they respond chaotically, and when they like to synchronize *Neurosci. Res.* **36** 81–91
[22] Stoop R, Schindler K and Bunimovich L A 2000 Neocortical networks of pyramidal neurons: from local locking and chaos to macroscopic chaos and synchronization *Nonlinearity* **13** 1515–29
[23] Maistrenko Y L, Popovych O, Burylko O and Tass P A 2004 Mechanism of desynchronization in the finite-dimensional Kuramoto model *Phys. Rev. Lett.* **93** 084102
[24] Maistrenko Y L, Popovych O V and Tass P A 2005 Desynchronization and chaos in the Kuramoto model *Lect. Notes Phys.* **671** 285–306
[25] Martignoli S and Stoop R 2008 Phase-locking and Arnold coding in prototypical network topologies *Discrete Cont. Dyn-B* **9** 145–62
[26] Cao H and Wu Y 2013 Bursting types and stable domains of Rulkov neuron network with mean field coupling *Int. J. Bifurcat. Chaos* **23** 1330041
[27] Wiggins S 2003 *Introduction to Applied Nonlinear Dynamical Systems and Chaos* (Berlin: Springer)
[28] Rasband S N 1989 *Chaotic Dynamics of Nonlinear Systems* (New York: Wiley)
[29] Grebogi C, Ott E and Yorke J A 1982 Chaotic attractors in crisis *Phys. Rev. Lett.* **48** 1507
[30] Viana R L, Batista A M, Batista C A S, Pontes J C A, Silva F A S and Lopes S R 2012 Bursting synchronization in networks with long-range coupling mediated by a diffusing chemical substance *Commun. Nonlinear Sci. Numer. Simul.* **17** 2924–42
[31] Yu H *et al* 2011 Chaotic phase synchronization in small-world networks of bursting neurons *Chaos* **21** 013127
[32] Batista C A S, Batista A M, Pontes J C A, Lopes S R and Viana R L 2009 Bursting synchronization in scale-free networks *Chaos Soliton. Fract.* **41** 2220–5